# Two-Tier Interference Elimination for Femtocells Based on Cognitive Radio Centralized Spectrum Management

**Leng-Gan Yi and Yi-Min Lu**
Department of Electronics and Information Engineering, Huazhong University of Science and Technology
Wuhan 430074, P. R. China.
[e-mail: yilenggan@gmail.com, luym@mail.hust.edu.cn]
*Corresponding author: Leng-Gan Yi

*Received January 27, 2014; revised March 30, 2014; accepted April 7, 2014; published May 29, 2014*

## Abstract

Femtocell provides better coverage and higher spectrum efficiency in areas rarely covered by macrocells. However, serious two-tier interference emerging from randomly deploying femtocells may create dead zones where the service is unavailable for macro-users. In this paper, we present adopting cognitive radio spectrum overlay to avoid intra-tier interference and incorporating spectrum underlay and overlay to coordinate cross-tier interference. It is a novel centralized control strategy appropriate for both uplink and downlink transmission. We introduce the application of proper spectrum sharing strategy plus optimal power allocation to address the issue of OFDM-based femtocells interference-limited downlink transmission, along with, a low-complexity suboptimal solution proposed. Simulation results illustrate the proposed optimal scheme achieves the highest transmission rate on successfully avoiding two-tier interference, and outperforms the traditional spectrum underlay or spectrum overlay, via maximizing the opportunity to transmit. Moreover, the strength of our proposed schemes is further demonstrated by comparison with previous classic power allocation methods, in terms of transmission rate, computational complexity and signal peak-to-average power ratio.

***Keywords:*** Cognitive radio, femtocell, interference elimination, OFDM, power allocation, spectrum management

**http://dx.doi.org/10.3837/tiis.2014.05.001**

## 1. Introduction

Femtocells deliver wireless broadband services to the home or office customers with low-power transmission. The **femtocell base station** (FBS) often approaches very close to subscribers, resulting in signal-to-interference-plus-noise ratio (SINR) improved [1]. Overall network coverage and capacity have been enhanced, because of FBS generally deployed at the edge of the macrocell. Recently, due to effective infrastructure cost and better meeting users dominant indoor communication needs, both operators and academia desire to develop femtocell rapidly. In the early days of femtocells, many technical issues should be overcome, including the plug-and-play interoperability, synchronization and security, seamless handover, interference alleviation [2].

Universal frequency reuse, reuse factor of one, increases the long-term evolution (LTE) system spectral efficiency, but when femtocells deployed densely, inter-femtocell and femtocell-macrocell interference degrades the system performance [3]. Antenna sectoring and time hopping rather than spectrum splitting are employed to solve intra/cross-tier interference in uplink CDMA femtocell networks [4]. Interference management of power self-calibration and limitation, is proposed for 3G HSPA+ networks [5]. Six interference scenarios are elaborated in femtocell-macrocell heterogeneous networks, furthermore, reusing far-away users spectra and scheduling information to avoid strong interference are put forward [6]. Orthogonal radio resource allocation, a strategic game theory, decoding techniques and the Gibbs sampler are investigated to mitigate macro/femto interference [7]. Considering LTE employing orthogonal frequency division multiple access (OFDMA) downlink scheme, and to avoid burst interference resulting from random femtocell deployment, a new interference elimination clever manner is needed. In the paper, we introduce spectrum overlay and spectrum underlay simultaneously accessing, which further increase spectrum efficiency [8], plus power control to mitigate two-tier interference.

Cognitive radio [9] originating from the software defined radio is deemed as an effective technique to help nodes to be smartly aware of the surrounding radio electromagnetic environment [10]. Cognitive radio enabled femtocells opportunely access licensed spectrum bands such as macrocell and TV broadcast networks was presented [11]. However, they were concerned only with the downlink spectrum overlay sharing problem. Via each femto-base station autonomously sensing channels usage of the macrocell, stand-alone femtocell employs the unoccupied channels, collocated femtocells exploit strategic game to randomize the utilization of these channels to provide Quality-of-Service (QoS) guarantees transmission was proposed [12]. Cognitive radio inspired approaches including spectrum sensing, cluster-based femtocells dynamic frequency reuse, and cognitive relay node were presented for interference coordination [13]. However, the above three literature all choose distributive autonomous manner, which cannot sidestep three problems: (i) Without the locations of moving macro-users, it is very hard work for femto-base station to sense the unoccupied channels. (ii) Facing one vicinal macro-user, a number of femotcells have to repeat difficult sensing tasks. (iii) Selfish femtocell individually allocating spectrum based on local information cannot avoid intra-tier interference completely. So FBSs provided with cognitive capability [14] assisted the necessary information from the **macrocell base station** (MBS) via backhaul link obeying the MBS centralized spectrum management is an alternative interference-mitigation solution.

The major contributions of this article include: 1) We first explicitly point out centralized cognitive spectrum overlay and underlay (spectrum two-lay) management can effectively

mitigate two-tier femtocell interference. 2) We introduce an optimal power control algorithm employing cognitive spectrum two-lay mode to fulfill OFDM-based femtocells effective downlink transmission, and address a low-complexity considerable-rate suboptimal scheme based on water-filling method. 3) We evaluate the performance of the proposed schemes by extensive simulation.

The rest of the paper is organized as follows. Section 2 details the role of cognitive spectrum two-lay access in femtocell interference mitigation. Section 3 describes the model of OFDM-based femtocells downlink two-tier interference. In Section 4, an optimal power allocation approach based on cognitive radio spectrum management and a suboptimal solution are proposed. Section 5 presents schemes comparisons. Section 6 gives extensive simulations to evaluate the performance of our proposed schemes and the conclusion is drawn in Section 7.

## 2. Spectrum Two-lay Models Coping with Two-Tier Interference

LTE is intended to operate with a universal frequency reuse geared to higher throughput, where any cells share the identical set of frequencies. Although spectral efficiency maximized, two-tier femtocell interference appears. Co-layer interference, i.e. intra-tier interference is described as the unnecessary signal sent from a femtocell and received at other femtocells. Cross-tier interference is the aggressor and the victim of interference belonging to different layers such as macrocell and femtocell. Early cellular concept was the first breakthrough in obtaining higher user capacity and interference avoidance between mobile users, relying on frequency reuse. Nowadays, the macrocell overlaid with femtocells complicates the problem.

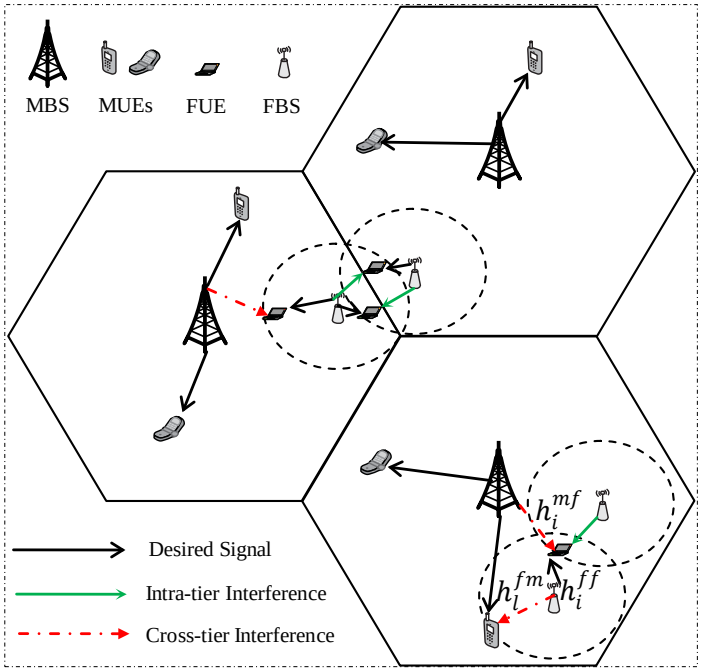


**Fig. 1.** Downlink two-tier interference under universal frequency reuse

Dynamic spectrum access to cognitive radio networks is classified as two types, underlay and overlay. In the spectrum underlay, secondary users are allowed to concurrently transmit

with primary users, only if the co-channel interference is limited to below the interference temperature threshold first presented by the FCC, which results in higher spectrum utilization. Secondary users temporarily occupy the licensed spectrum, only when the primary users are absent, that is the spectrum overlay mode, like time or frequency division multiplexing.

Facing the femtocell two-tier interference challenge due to the lack of coordination, we present cognitive radio spectrum two-lay management to solve. In short, femotcell and marcocell run in spectrum sharing mode and femotcells opportunistically access to cognitive marcocell networks. To increase spectral efficiency, LTE femotcells simultaneously operate in licensed spectrum with macrocell, so that cross-tier interference is inevitable. Fortunately, in the spectrum underlay, cross-tier interference is diminished under the interference temperature threshold so much so that they suffer no harmful interference, which is naturally equivalent to interference avoidance. Specifically, the interference is weak, where co-channel femto-users are far away from macro-users of the identical macrocell. Certainly, it is better macrocell and femtocell running in the spectrum overlay, interference-free, thanks to signals orthogonalization. Femotcell is characterized by low-power short-range coverage, so mutual interference among femotcells usually does not occur. Even if femtocells are deployed densely, as long as femotcells operate in the spectrum overlay, intra-tier interference vanishes due to assigning non-overlapping channels. In conclusion, agilely using spectrum two-lay can completely remove two-tier femtocell interference, as long as the cognitive radio spectrum management is powerfully implemented. Note that the interference avoidance scheme is suitable for uplink and downlink transmission, even with different multiple access technology.

## 3. System Model and Formulation

Femtocell networks downlink two-tier interference scenarios are shown in **Fig. 1**. Macrocell coverage area is represented by Hexagon. Dashed circle shows femtocell coverage area, where the **macrocell user** (MUE) and the **femtocell user** (FUE) can coexist. The solid green line arrowhead and the dotted red line arrowhead denote intra-tier interference and cross-tier interference, respectively.

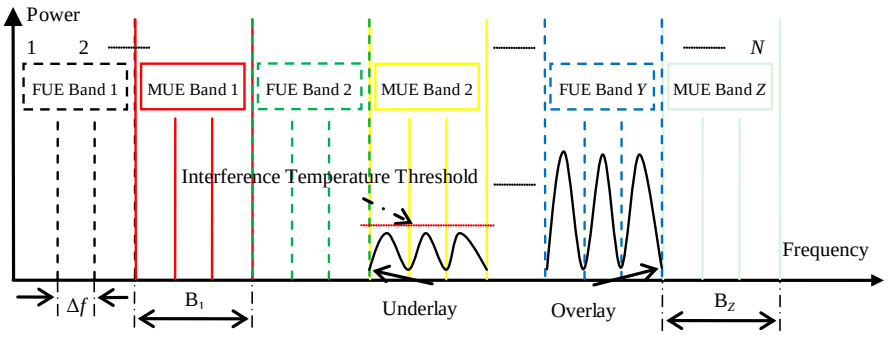


**Fig. 2.** Spectrum two-lay power allocation according to distribution of MUEs

The research is built on the model described in [15]. The entire frequency band is divided into $N$ subcarriers, each interval is $\Delta f$ Hz, as shown in **Fig. 2.** The $Z$ MUEs have occupied $B_1$, $B_2$, …, $B_Z$ bandwidth, so spectrum underlay FUEs are allocated power forcedly below the interference temperature threshold to ensure the desired QoS to these MUEs. Via four methods include centralized notification, server part information sensing, server blind sensing and

distributed assistant sensing, the FBS knows three instantaneous Rayleigh fading channel gains [14]: $h_i^{mf}$ representing the downlink channel gain from MBS to FUE, $h_l^{fm}$ indicating the one from FBS to MUE, between the FBS and FUE, denoted as $h_i^{ff}$, illustrated in **Fig. 1**.

As aforementioned, femtocell intra-tier interference does not occur in the spectrum overlay model, the following sections focus on femtocell cross-tier interference.

### 3.1. Cross-Tier Interference Introduced by FBS

Given OFDM employing the rectangular non-return-to-zero (NRZ) signal [15], the power density spectrum (PDS) of the $i$-th subcarrier is defined as [16], [17]

$$\Phi_i(f) = P_i T_s \left(\frac{sin\ \pi f T_s}{\pi f T_s}\right)^2, \tag{1}$$

where $P_i$ denotes the $i$-th subcarrier transmit power. $T_s$ is the symbol duration, $T_s = 1/\Delta f$ +guard interval [15]. The FBS interfering to MUE $l$-th subcarrier, denoted as $I_{F\to M}(P_i, l)$, the sum of all subcarriers integration of the PDS, is written as

$$I_{F\to M}(P_i, l) = \sum_{i=1}^{N} |\, h_l^{fm}|^2 \int_{(d_{il}-1/2)\Delta f}^{(d_{il}+1/2)\Delta f} \Phi_i\,(f) df, \tag{2}$$

where $d_{il}$, an integer, denotes the distance between $i$-th subcarrier of FBS and $l$-th subcarrier of MUE. $h_l^{fm}$ is the FBS to MUE $l$-th subcarrier channel gain. Let $\mathbf{O}$, $L$ denote the set of the total occupied subcarriers, the total number of spectrum underlay subcarriers, respectively. Then the cardinality of the set $\mathbf{O}$ is $L$, i.e., $|\mathbf{O}| = L$. **Note that** the interference $I_{F\to M}(P_i, l)$ includes FBS both spectrum overlay and spectrum underlay transmissions impact, because it is the sum of total $N$ subcarriers, either occupied by MUEs, i.e., $i \in \mathbf{O}$ or unoccupied, i.e., $i \in \mathbf{U} = \{x | x \in \{1,2,\cdots,N\}, x \notin \mathbf{O}\}$.

### 3.2. Cross-Tier Interference Introduced by MBS

Assuming a rectangular window function used [15], the PDS of MBS signal after M-fast Fourier transform (FFT) processing can be given as [15], [16]

$$E\{I_M(\omega)\} = \frac{1}{2\pi M} \int_{-\pi}^{\pi} \Phi_{\mathrm{MBS}}\,(e^{j\omega}) \left(\frac{sin(\omega-\psi)M/2}{sin(\omega-\psi)/2}\right)^2 d\psi, \tag{3}$$

where $\omega$ signifies the normalized frequency, $\Phi_{\mathrm{MBS}}(e^{j\omega})$ stands for the PDS of MBS signal before M-FFT. The MBS interfering to FUE $i$-th subcarrier, denoted as $I_{M\to F}(i)$, sum of all $l$-th subcarrier integration of the PDS, is written as

$$I_{M\to F}(i) = \sum_{l=1}^{L} |\, h_i^{mf}|^2 \int_{(d_{il}-1/2)\Delta f}^{(d_{il}+1/2)\Delta f} E\,\{I_M(\omega)\} d\omega. \tag{4}$$

where $L$ signifies the total number of subcarriers occupied by MUEs. $h_i^{mf}$ is the MBS to FUE $i$-th subcarrier channel gain.

## 4. Cognitive Radio Centralized Spectrum Management for Interference Mitigation

We think efficiently coexisting with macrocell to provide FUEs reliable communication without harmful interference, femtocells need cognitive radio assistance. To achieve the goal, three fundamental cognitive tasks must be addressed [10]:

- Radio-scene analysis.
- Channel-state estimation and predictive modeling.
- Transmit-power control and dynamic spectrum management.

The first two tasks can be fulfilled through a variety of approaches. In this paper, we advocate non-subscriber-terminal spectrum sensing [14], and centralized coordination to assist estimating channel state. The MBS provide necessary information to the FBS through backhaul link: 1) the near MUEs' location information to help get channel gain $h_l^{fm}$ and their occupied subcarriers, 2) cross-tier interference to FUEs i.e., $I_{M\to F}(i)$, 3) neighbor FBSs of together spectrum overlay accessing, 4) the interference threshold these MUEs can endure, according to their QoS demand. The first three jobs depending only on sensing are so difficult, that the coordination plays the important role in interference avoidance. Next, we mainly focus on the third task: multiple-access control, i.e. transmit-power control plus dynamic spectrum management [10]. Our goal is to allocate maximum power to the best available frequency band to meet FUEs high-rate requirement. We hope to obtain the most suitable spectrum utilization, however, if MUEs' interference threshold is strictly controlled, handy option is to allow only overlay spectrum access rather than to manage two-lay spectrum bands.

### 4.1. The Proposed Optimal Scheme

The objective is to adjust each subcarrier power to maximize femtocell downlink throughput $R$, on the premise of curbing two-tier interference.

$$\max_{P_i} R = \max_{P_i} \sum_{i=1}^{N} \Delta f \log_2 \left(1 + \frac{|h_i^{ff}|^2 P_i}{\sigma^2 + I_{M\to F}(i)}\right), \tag{5}$$

subject to,

$$\sum_{l=1}^{L} I_{F\to M}(P_i, l) \le I_{th}, \tag{6}$$

$$\sum_{i=1}^{N} P_i \le P_T, \tag{7}$$

$$P_i \ge 0, \ \forall \ i = 1,2,\cdots,N, \tag{8}$$

where $h_i^{ff}$, $P_i$ denote the FBS to FUE $i$-th subcarrier channel gain, transmit power, respectively. $\sigma^2$ represents the additive white Gaussian noise. $P_T$ is the transmission power budget. $I_{th}$ signifies the interference temperature threshold. The second derivative of $R$ with regards to $P_i$ can be derived as

$$\nabla_{P_i}^2 R = \frac{\Delta f |h_i^{ff}|^4}{\ln(2)(\sigma^2 + I_{M\to F}(i) + |h_i^{ff}|^2 P_i)^2} > 0, \forall P_i.$$

Hence, the problem formulation is convex, so the duality gap is zero.

Since the $\Delta f$ remains constant, it can be omitted in the calculation, for simplicity, so optimal power is written as $P_i^* = \arg\max(R) = \arg\min(-\sum_{i=1}^{N}\log_2(1+\frac{|h_i^{ff}|^2 P_i}{\sigma^2+I_{M\to F}(i)}))$. Therefore, relaxing the constraints in (6)-(8), the Lagrangian is represented as

$$\begin{aligned} L(P_i,\lambda_1,\lambda_2,\lambda_3) &= -\sum_{i=1}^{N}\log_2\left(1+\frac{|h_i^{ff}|^2 P_i}{\sigma^2+I_{M\to F}(i)}\right) \\ &+\lambda_1\left(\sum_{l=1}^{L} I_{F\to M}(P_i,l)-I_{th}\right)+\lambda_2\left(\sum_{i=1}^{N}P_i-P_T\right)-\lambda_3 P_i, \end{aligned} \tag{9}$$

where $\lambda_1$, $\lambda_2$ and $\lambda_3$ are Lagrange multipliers. Based on the Karush-Kuhn-Tucker (KKT) conditions [18] as follows

$$\begin{aligned} &P_i^* \geq 0, \ \forall\ i=1,2,\cdots,N, \\ &\sum_{l=1}^{L} I_{F\to M}(P_i^*,l)-I_{th}\leq 0, \ \forall\ i=1,2,\cdots,N, \\ &\sum_{i=1}^{N} P_i^*-P_T\leq 0, \ \forall\ i=1,2,\cdots,N, \\ &\lambda_w^*\geq 0, \ \forall\ w=1,2,3, \\ &\lambda_1^*\left(\sum_{l=1}^{L} I_{F\to M}(P_i^*,l)-I_{th}\right)=0, \forall\ i=1,2,\cdots,N, \\ &\lambda_2^*\left(\sum_{i=1}^{N} P_i^*-P_T\right)=0, \ \forall\ i=1,2,\cdots,N, \\ &\lambda_3^* P_i^*=0, \ \forall\ i=1,2,\cdots,N, \\ &\nabla_{P_i} L(P_i^*,\lambda_1^*,\lambda_2^*,\lambda_3^*)=0, \ \forall\ i=1,2,\cdots,N. \end{aligned} \tag{10}$$

Since $P_i^*\geq 0$, so $\lambda_3^*=0$, the optimal power value is yielded

$$P_i^* = \left[\frac{1}{\ln(2)(\lambda_1 G+\lambda_2)}-\frac{\sigma^2+I_{M\to F}(i)}{|h_i^{ff}|^2}\right]^+, \tag{11}$$

where $G=\sum_{l=1}^{L}|h_l^{fm}|^2 T_s\int_{(d_{il}-1/2)\Delta f}^{(d_{il}+1/2)\Delta f}\left(\frac{\sin \pi f T_s}{\pi f T_s}\right)^2 df$, $[\cdot]^+=\max\{\cdot,0\}$. Derived from subgradient method, $\lambda_1$, $\lambda_2$ are updated, respectively, as

$$\lambda_1^{k+1} = \left[\lambda_1^k+\alpha^k\left(\sum_{l=1}^{L} I_{F\to M}(P_i,l)-I_{th}\right)\right]^+, \tag{12}$$

$$\lambda_2^{k+1} = \left[\lambda_2^k+\beta^k\left(\sum_{i=1}^{N} P_i-P_T\right)\right]^+. \tag{13}$$

**Algorithm 1** Calculate $P_i^* = \arg\max(R)$

Initialize $\lambda_1^0$, $\lambda_2^0$, $\alpha^0$, $\beta^0$;
**While** non-convergence **do**
  Compute $P_i^k$ according to (11);
  Update $\lambda_1^k$ according to (12);
  Update $\lambda_2^k$ in the light of (13).
**End while**

Note that as long as k is large enough, it guarantees the algorithm accurately converges to the optimal value. The time complexity of the core algorithm is $\mathcal{O}(KNL)$, where $K$, $N$, $L$ are the total number of iterations, of subcarriers, of subcarriers occupied by MUEs, respectively. The variable $K$ is determined by convergence precision and the initial values $\lambda_1^0$, $\lambda_2^0$, $\alpha^0$, $\beta^0$.

In spectrum overlay, the left of (6) is always less than the right, according to the KKT conditions, $\lambda_1^* = 0$. However, the right of (7) is permanently greater than the left in spectrum underlay, so $\lambda_2^* = 0$. Therefore the algorithm accomplishes spectrum two-lay optimal power allocation, combating two-tier femtocell interference.

### 4.2. The Proposed Suboptimal Scheme

Based on the heuristic that when interference threshold $I_{th}$ is stringent, spectrum overlay outperforms spectrum two-lay in total rates in non-optimization approaches, we proposed a low-complexity suboptimal scheme. The key idea is that according to the model switching threshold $M_{th}$, determined by the total power budget $P_T$, we choose the proper classic water-filling scheme as the suboptimal power profile, which can be expressed as

$$P_i^{SO} = \begin{cases} P_i^{WF}, & i \in \mathbf{U}, \quad \text{if} \quad M_{th} \geq I_{th}; \\ P_i^{WF}, & i \in \{1,2,\dots,N\}, \quad \text{if} \quad M_{th} \leq I_{th}. \end{cases}$$

Where $P_i^{WF}$**,** denoted as water-filling subcarrier power allocation, which is elaborated in subsection 5.3. The **U** is the set of the subcarriers unoccupied, defined in subsection 3.1.

**Proposition 1.** *Given $P_T$, the model switching threshold satisfies $M_{th} = \frac{((1+\frac{A \cdot P_T}{N-L})^{\frac{N-L}{N}} - 1) \cdot \sum_{i=1}^{N} G}{A}$, where $A = E\left(\frac{|h_i^{ff}|^2}{\sigma^2 + I_{M \to F}(i)}\right)$,$G$ is derived in section 4.1. $E(\cdot)$ denotes the expectation operator.*

*Proof.*

Please refer to Appendix. ■

Note that when the channel gains of each subcarrier do not vary, the equal power allocation is a special case of the water-filling method, so we adopt water-filling power assignment as the core algorithm of the suboptimal scheme.

## 5. Schemes Comparison

In order to better show the superiority, we selected four representative algorithms to do comparison with optimal and suboptimal algorithms.

### 5.1. Sequential Quadratic Programming Scheme

As we all know, (5)-(8) form a Nonlinear Programming Problem (NLP). In past years, via the linearization of the actual constraints about $P_i$ in (6)-(8), the above NLP can be solved by finding the minimum value $d_{P_i}$ in the Sequential Quadratic Programming (SQP) as [19]

$$\min_{d_{P_i}} \nabla_{P_i}(-R(P_i^k))d_{P_i} + \frac{1}{2} d_{P_i} \nabla_{P_i}^2 L(P_i^k, \lambda_1^k, \lambda_2^k) d_{P_i},$$

subject to,

$$C_1(P_i^k) + \nabla_{P_i} C_1(P_i^k) d_{P_i} \le 0,$$
$$C_2(P_i^k) + \nabla_{P_i} C_2(P_i^k) d_{P_i} \le 0,$$

where $C_1(P_i^k) = \sum_{l=1}^{L} I_{F\to M}(P_i^k, l) - I_{th}$, $C_2(P_i^k) = \sum_{i=1}^{N} P_i - P_T$. When setting $\lambda_1^{k+1} = \lambda_1^k + \eta d_{\lambda_1^k}$ and $\lambda_2^{k+1} = \lambda_2^k + \eta d_{\lambda_2^k}$, which $\eta$, $d_{\lambda_1^k}$ and $d_{\lambda_2^k}$ are chosen to satisfy the KKT optimality conditions, the SQP can be solved by Newton' s method [18]. A similar optimal scheme was used in [17], which is denoted as SQPS here. Although the complexity of the SQPS scheme is also $\mathcal{O}(KNL)$, the Hessian of the Lagrangian, however, should be computed in each iterative. Furthermore, if the Newton decrement [18] is used as stopping criterion, the total number of iterations $K$ is always larger than the one in our proposed optimal scheme.

### 5.2. Ladder Fashion Proportion Scheme

Since major cross-tier interference results from spectrum underlay transmission, so a reasonable strategy is to allocate more power to the idle subcarriers, taking advantage of the overlay model. The authors in [17] introduced Ladder Fashion Proportion scheme (LFPS) to simply fulfill power allocation. They assume equal power values are assigned to the underlay subcarriers, i.e., $P_i = P_{underlay}$, $\forall\, i \in \mathbf{O}$. The minimum power value $\underline{P_{overlay}}$ allocated among the overlay subcarriers is an integral multiple of the $P_{underlay}$. According to the minimum distance $d$ between overlay subcarriers and underlay subcarriers, the power distribution of the overlay subcarriers takes a ladder fashion profile, i.e., $P_i = d \cdot \underline{P_{overlay}}$, $\forall\, i \in \mathbf{U}$ in their design. Note that $\mathbf{O}$ and $\mathbf{U}$ are sets defined in Section 3.1. It is easier work to find proper $P_{underlay}$ satisfying both power and interference constraints, so that the complexity of the LFPS scheme is $\mathcal{O}(NL)$, due to no iteration required.

### 5.3. Classical Water-filling Scheme

The well-known water-filling scheme can optimize the power distribution over multi-carrier transmission, due to taking advantage of the better channel conditions, i.e., more power allocated to the stronger subcarriers. A linear water-filling algorithm for delay-tolerant users multi-media service allocation was presented [20]. Here, the precise formulation is written as $P_i^{WF} = \left[\frac{1}{\mu} - \frac{\sigma^2 + I_{M\to F}(i)}{|h_i^{ff}|^2}\right]^+$, where the water-filling level $\frac{1}{\mu}$ is a constant chosen so that the power and interference threshold constraints are met. Note that when $i \in \mathbf{U}$, the scheme only considers spectrum overlay model, when $i \in \{1,2,\ldots,N\}$, water-filling two-lay power allocation comes into being.

### 5.4. Classical Equal Power

The simplest solution is equal power allocation, because it does not consider the change of

channel gains. The minimum equal power value should be chosen as it satisfies both the constraints (6)-(7). As above, there are two modes, i.e., spectrum overlay equal power allocation and equal power two-lay model.

The complexity comparison of different schemes is concluded, as shown in **Table 1**.

**Table 1.** Algorithm Complexity Comparison

| Algorithm | Complexity |
|---|---|
| Proposed Optimal | $\mathcal{O}(KNL)$ |
| Proposed Suboptimal | $\mathcal{O}(NL)$ |
| SQPS | $\mathcal{O}(KNL)$ |
| LFPS | $\mathcal{O}(NL)$ |
| Classical Water-filling | $\mathcal{O}(NL)$ |
| Classical Equal Power | $\mathcal{O}(NL)$ |

The high peak-to-average power ratio (PAPR), defined as the ratio between the maximum instantaneous power and its average power, leads to nonlinear distortion, requiring high-resolution digital-analog converter and high power amplifier to handle, which limits the OFDM applications [21]. So it is essential to compare the PAPR among several schemes.

## 6. Numerical Results

We consider the scenario that 3 MUEs are present to occupy $L = 10$ subcarriers, among total subcarriers $N = 32$; and set the OFDM symbol duration $T_s = 4\,\mu s$, subcarrier interval $\Delta f = 0.3125$ MHz, the additive white Gaussian noise $\sigma^2 = 10^{-5}$, the transmission power budget $P_T = 10^{-3}$ W. We assume $h_i^{ff}$, $h_l^{fm}$ Rayleigh fading channel gain average values as 6 dB, 3 dB. The average value of $I_{M\to F}(i)$ is fixed as $10^{-4}$ W, then varies from $10^{-4}$ to $9 \cdot 10^{-4}$, simplified as $I_{M\to F}$ in the following.

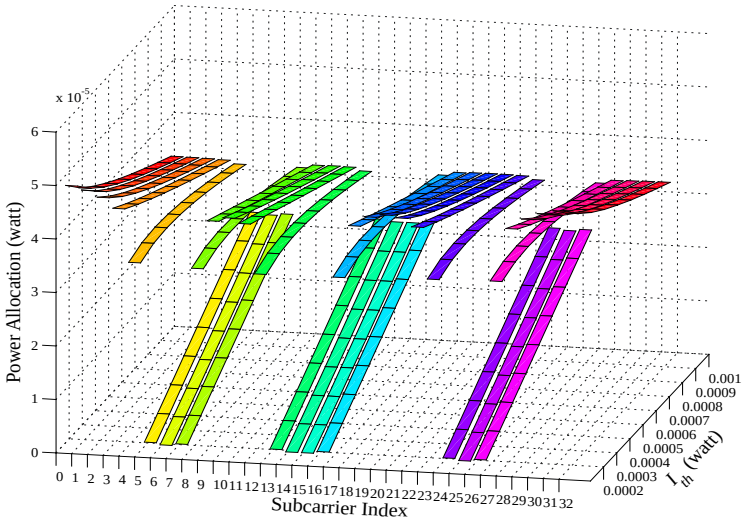


**Fig. 3.** Optimal multi-subcarrier power allocation according to the distribution of MUEs versus cross-tier interference threshold $I_{th}$

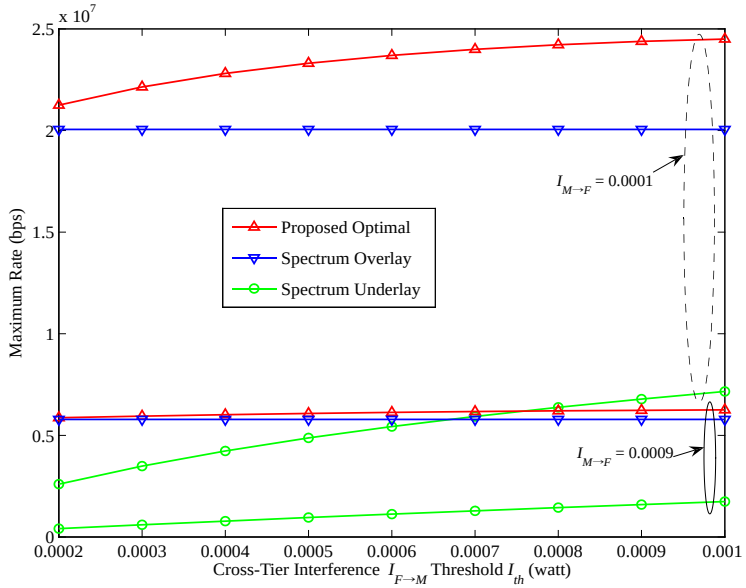


**Fig. 4.** Comparison of maximum rate versus cross-tier interference threshold $I_{th}$ among the proposed optimal and spectrum overlay and underlay

In **Fig. 3**, FUEs spectrum two-lay optimal power allocation according to the distribution of MUEs is studied by varying cross-tier interference threshold $I_{th}$ from $2 \cdot 10^{-4}$ to $10^{-3}$, where $I_{M \to F} = 10^{-4}$. **Fig. 3** shows subcarrier power of FUEs spectrum underlay significantly reduces, as the $I_{th}$ reduces, which implies the proposed optimal algorithm effectively controls cross-tier interference; on the other hand, the power of spectrum overlay obviously raises in order to spend the transmission power budget. Clearly, power is loaded at every subcarrier, the higher for spectrum overlay, $3.3 \cdot 10^{-5} < P_i^{overlay} < 5.1 \cdot 10^{-5}$, the lower for spectrum

underlay, $2 \cdot 10^{-6} < P_i^{underlay} < 2.7 \cdot 10^{-5}$, which indicates the proposed optimal performs spectrum two-lay management. Since the restriction (6) controls the sum of all subcarriers interference, therefore, underlay subcarriers assigned power forms a smaller inverted triangle along the ordinate. Conversely, power distribution of spectrum overlay shows a larger triangle; in which, the nearer to MUEs subcarrier, the growth trend is smaller, the others present bigger ladder growth. Just as expected, from interference-limited perspective, **Fig. 3** illustrates the maximum power is allocated to the best available subcarrier.

**Fig. 4** demonstrates the maximum rate increases, as cross-tier interference threshold $I_{th}$ raises from $2 \cdot 10^{-4}$ to $10^{-3}$, and the growth trend is visible when $I_{M \to F} = 10^{-4}$. It reveals that as the $I_{th}$ rises, i.e. the QoS demand for MUEs declines, FUEs have the opportunity to obtain a higher rate. **Fig. 4** shows that the proposed optimal scheme outperforms only spectrum overlay and only spectrum underlay, and such advantage is clearer under slighter $I_{M \to F}$; because the former loads power on each subcarrier, but the latter abandons some subcarriers, which hints transmission rate maximization benefits from access opportunity maximization. As the $I_{th}$ reduces, the gap between the proposal and spectrum overlay gets narrower, which implies the advantage of the former, i.e. partly using spectrum underlay, becomes puny, and the trend is distinct when $I_{M \to F} = 9 \cdot 10^{-4}$. The spectrum overlay model unlikely violates the threshold $I_{th}$, so the curve is a straight line, because $\lambda_1^* = 0$, which is explained in subsection 4.1, the power values of the subcarriers unoccupied by the MUEs do not change as the $I_{th}$ changes.

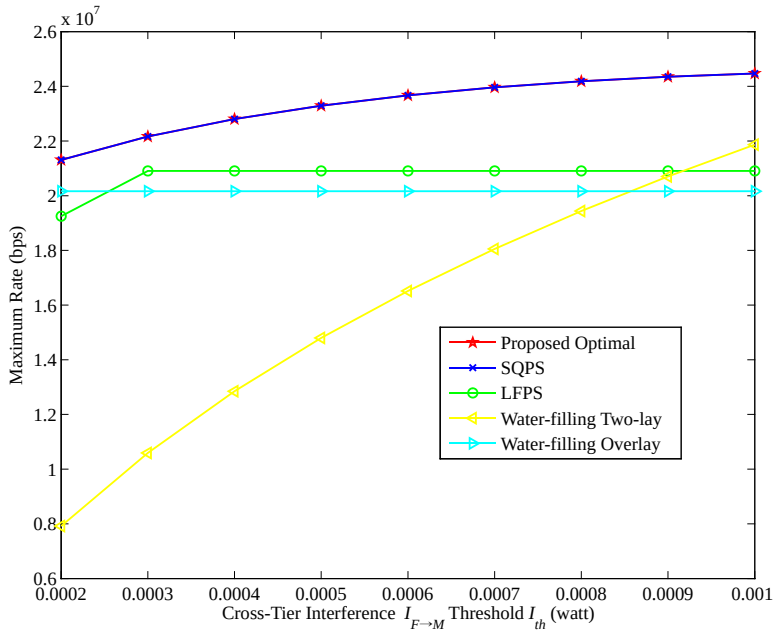


(a) Proposed optimal scheme comparison

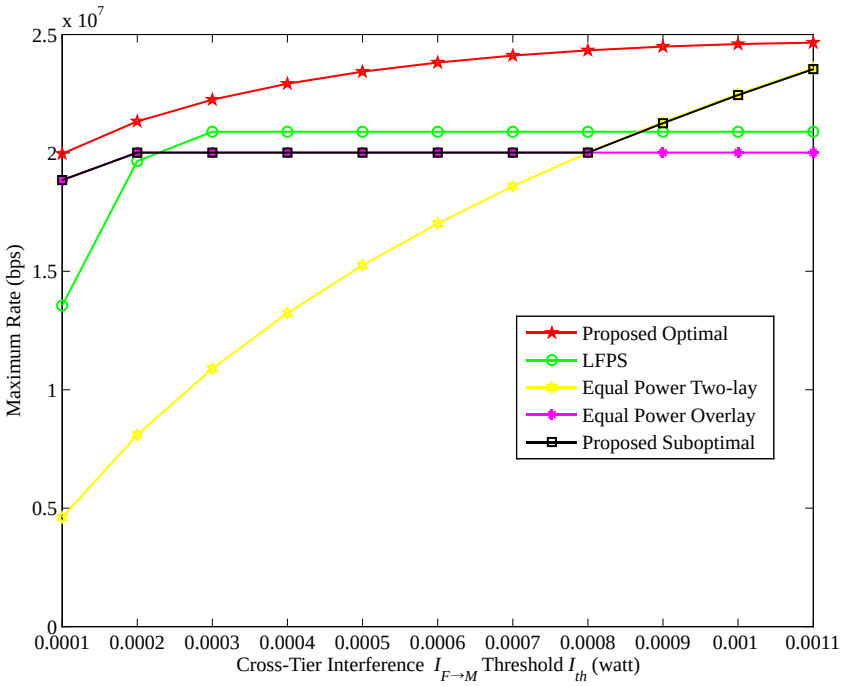


(b) Proposed suboptimal scheme comparison

**Fig. 5.** Comparison with classical schemes

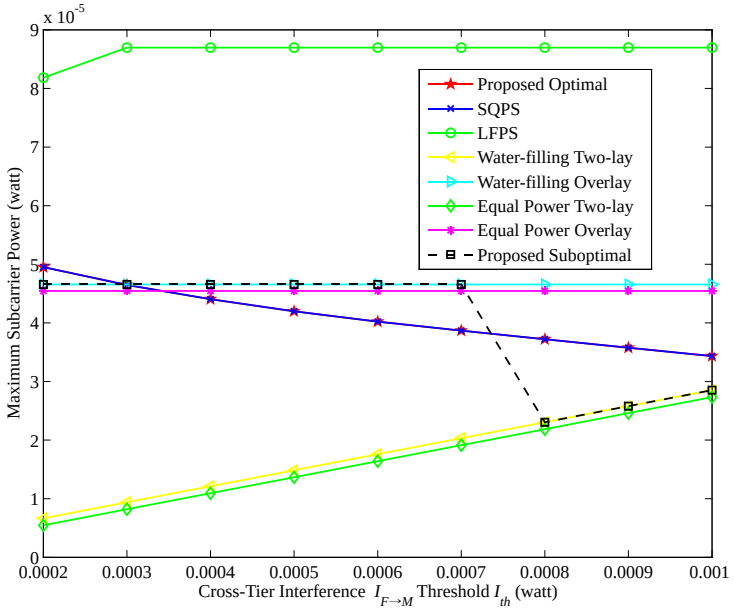


(a) Maximum subcarrier power comparison

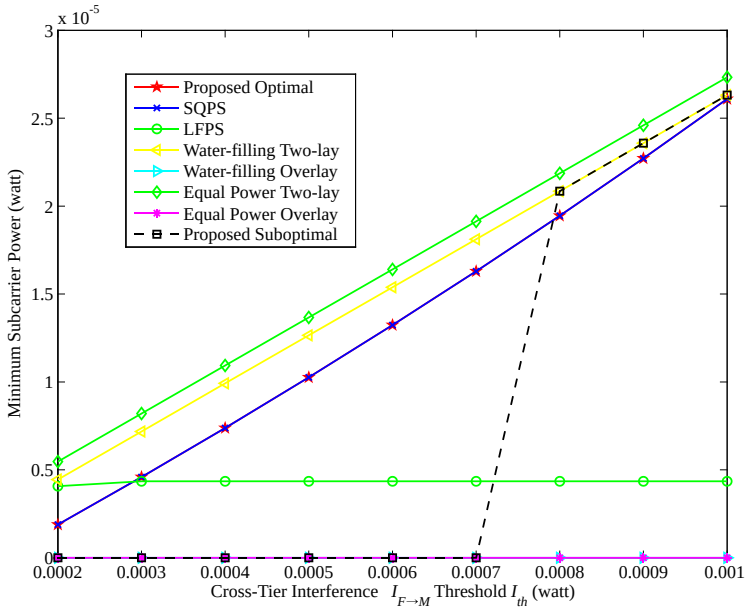


(b) Minimum subcarrier power comparison

**Fig. 6.** Subcarrier power comparison among different schemes

**Fig. 5** presents maximum transmission rate versus cross-tier interference threshold $I_{th}$ when $I_{M\to F} = 10^{-4}$, where proposed optimal and suboptimal schemes are compared with the SOPS, the LFPS, classic water-filling and equal power methods. We observe that the proposed optimal and the SOPS achieve highest performance, at the expense of more time optimization calculation, and when $I_{th}$ increases, the growth trends coincide. The optimal is superior to the water-filling overlay scheme at least 1 Mbps rate increase, as shown in **Fig. 5(a)**, and water-filling underlay performs poorly, given interference controlled strictly, which indicates simple two-lay spectrum access without optimization is not desirable. Fig. 5(b) shows the proposed suboptimal outperforms the LFPS scheme, especially when $I_{th}$ is small enough or large enough. From two sub-figures, we surprisingly find 1) although each subcarrier power values differ, classic equal power and water-filling rate outcomes are of equivalent, and 2) their two-lay power allocation results are inferior to their overlay design, when $I_{th}$ is small, due to the interference threshold constraint (6) severely restricts the maximum subcarrier power, as shown in **Fig. 6(a)**.

**Fig.6** reveals two extreme power values of $N$ subcarriers, as the cross-tier interference threshold $I_{th}$ increases, when $I_{M\to F} = 10^{-4}$. Combine the information in two sub-figures, we highlight six points. First, the curves of two classic methods in overlay model present straight line. Second, there is difference in subcarrier power allocation between water-filling and equal power methods, no matter whether overlay or two-lay. Third, the maximum and minimum power values of the proposed optimal and suboptimal schemes elastically change, when $I_{th}$ raises. Fourth, the LFPS power allocation does not vary, when $I_{th}$ increases over $3 \cdot 10^{-4}$. Fifth, the proposed suboptimal power profile coincides with the water-filling scheme. Sixth, the maximum power value of the optimal scheme decreases, meanwhile, the minimum power value increases, given interference threshold grows, as shown in Fig. 3.

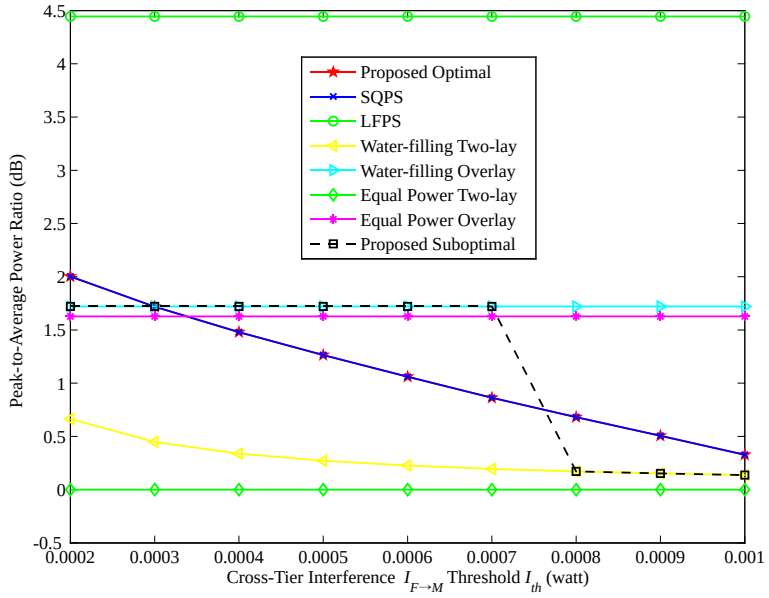


**Fig. 7.** PAPR comparison among different schemes

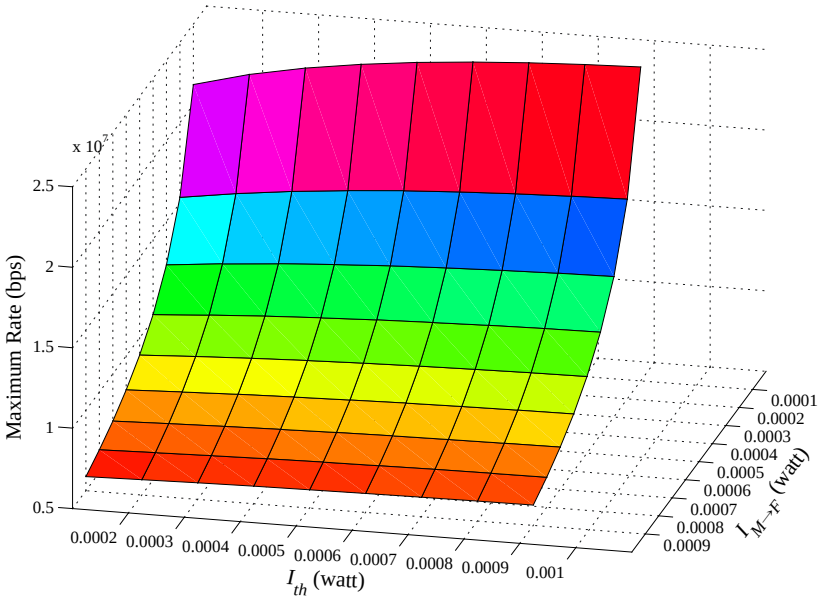


**Fig. 8.** Maximum rate versus $I_{th}$ and cross-tier interference $I_{M\to F}$

**Fig. 7** demonstrates the comparison of the PAPR of OFDM signal among different schemes versus cross-tier interference threshold. We observe that the LFPS has a shortcoming in the PAPR, which keeps more than 2 times higher than the others, and does not change, as $I_{th}$ increases. By contrast, equal power allocation in all subcarriers naturally outcomes zero PAPR. The proposed optimal and suboptimal schemes result in moderate PAPR. In brief, the proposed suboptimal scheme characterizes low-PAPR, considerable-rate, low-complexity and taking advantage of the better subcarriers channel condition.

**Fig. 8** illustrates the maximum rate varies, as the interference threshold $I_{th}$ raises from $2 \cdot 10^{-4}$ to $10^{-3}$, and cross-tier interference $I_{M\to F}$ declines from $9 \cdot 10^{-4}$ to $10^{-4}$. We observe that as $I_{th}$ increases, where $I_{M\to F} = 10^{-4}$, the throughput increases more than 3 Mbps, which implies although the power budget $P_T$ keeps constant, the data rate has increased, thanks to multi-carrier transmission. Because there are more subcarriers using the larger power to transmit. **Fig. 8** also shows that when the $I_{M\to F}$ turns into serious, the transmission data rate drops greatly, from more than 24.4 Mbps to less than 5.9 Mbps, the former is four times the latter, which well illustrates cross-tier interference undesired impact.

Note that the disturbing cross-tier interference $I_{M\to F}$ is treated as noise in the proposed scheme. Predictably, a similar approach should be used in MBS to restrict the $I_{M\to F}$. Therefore it becomes a more effective solution.

## 7. Conclusion

Femtocell two-tier interference mitigation using cognitive radio spectrum two-lay models has been addressed. A downlink throughput maximization algorithm fulfilling spectrum two-lay power allocation under the restrictions of the cross-tier interference and a low-complexity suboptimal scheme have been proposed. Presented extensive numerical results show the proposed optimal outperforms several classic schemes and traditional spectrum overlay or spectrum underlay in transmission rate, because of maximizing the utilization of multi-subcarrier transmission. Moreover, the suboptimal approach characterizes considerable-rate, low-PAPR, low-complexity, for being hybrid water-filling scheme of spectrum overlay and spectrum two-lay. However, these schemes all base on the perfect channel state information, i.e., the assumption of the first two steps in traditional cognitive cycle perfectly completed, here via reliable coordination between MBS and FBSs plus necessary information assisted sensing. Therefore, we consider future research includes robust spectrum sensing to eliminate femtocell two-tier interference under non-ideal coordination.

## Appendix

### Proof of the Proposition 1

Given power allocated to $N$ subcarriers, i.e., operating in spectrum two-lay model, the constraint (6) strictly restrains the water level, especially when $I_{th}$ is small, so that the water-filling two-lay scheme is inferior to water-filling overlay in the total rate. So we can find the model switching threshold $M_{th}$, when two scheme total rates are equivalent, i.e.,

$$\sum_{i=1}^{N} \Delta f \log_2\left(1+\frac{|h_i^{ff}|^2 P_i^{overlay}}{\sigma^2 + I_{M\to F}(i)}\right) = \sum_{i=1}^{N} \Delta f \log_2\left(1+\frac{|h_i^{ff}|^2 P_i^{two-lay}}{\sigma^2 + I_{M\to F}(i)}\right).$$

If we neglect the difference of channel gains and interference among all subcarriers, then we can get $(1 + A \cdot P_{eq}^{overlay})^{N-L} = (1 + A \cdot P_{eq}^{two-lay})^{N}$, where $A = E\left(\frac{|h_i^{ff}|^2}{\sigma^2 + I_{M\to F}(i)}\right)$. The $P_{eq}^{(\cdot)}$ denotes equal power value in different models. According to two constraints (6) and (7), we further yield $I_{th} = \frac{((1+\frac{A\cdot P_T}{N-L})^{\frac{N-L}{N}} - 1)\cdot \sum_{i=1}^{N} G}{A}$, fixed as the model switching threshold $M_{th}$. Proposition 1 is thus proved.

## References


[1] V. Chandrasekhar, J. G. Andrews and A. Gatherer, "Femtocell networks: a survey," *IEEE Communications Magazine*, vol.46, no.9, pp. 59-67, 2008. Article (CrossRef Link)

[2] R. Y. Kim, J. S. Kwak and K. Etemad, "WiMAX femtocell: requirements, challenges, and solutions," *IEEE Communications Magazine*, vol.47, no.9, pp. 84-91, 2009. Article (CrossRef Link)

[3] V. Chandrasekhar, J. G. Andrews, T. Muharemovic, Z. K. Shen and A. Gatherer, "Power control in two-tier femtocell networks," *IEEE Transactions on Wireless Communications*, vol.8, no.8, pp. 4316-4328, 2009. Article (CrossRef Link)

[4] V. Chandrasekhar and J. G. Andrews, "Uplink capacity and interference avoidance for two-tier femtocell networks," *IEEE Transactions on Wireless Communications*, vol.8, no.7, pp. 3498-3509, 2009. Article (CrossRef Link)

[5] M. Yavuz, F. Meshkati, S. Nanda, A. Pokhariyal, N. Johnson and B. Raghothaman, *et al.*, "Interference Management and Performance Analysis of UMTS/HSPA+ Femtocells," *IEEE Communications Magazine*, vol.47, no.9, pp. 102-109, 2009. Article (CrossRef Link)

[6] M. E. Sahin, I. Guvenc, M. Jeong and H. Arslan, "Handling CCI and ICI in OFDMA femtocell networks through frequency scheduling," *IEEE Transactions on Consumer Electronics*, vol.55, no.4, pp. 1936-1944, 2009. Article (CrossRef Link)

[7] S. M. Cheng, S. Y. Lien, F. S. Chu and K. C. Chen, "On exploiting cognitive radio to mitigate interference in macro/femto heterogeneous networks," *IEEE Wireless Communications*, vol.18, no.3, pp. 40-47, 2011. Article (CrossRef Link)

[8] Q. Zhao and B. M. Sadler, "A Survey of Dynamic Spectrum Access," *IEEE Signal Processing Magazine*, vol.24, no.3, pp. 79-89, 2007. Article (CrossRef Link)

[9] J. Mitola III, "Cognitive radio: An integrated agent architecture for software defined radio," Ph.D. dissertation, KTH Royal Institute of Technology, Stockholm, Sweden, 2000.

[10] S. Haykin, "Cognitive radio: Brain-empowered wireless communications," *IEEE Journal on Selected Areas in Communications*, vol.23, no.2, pp. 201-220, 2005. Article (CrossRef Link)

[11] J. Xiang, Y. Zhang, T. Skeie and L. Xie, "Downlink Spectrum Sharing for Cognitive Radio Femtocell Networks," *IEEE Systems Journal*, vol.4, no.4, pp. 524-534, 2010. Article (CrossRef Link)

[12] S. Y. Lien, Y. Y. Lin and K. C. Chen, "Cognitive and Game-Theoretical Radio Resource Management for Autonomous Femtocells with QoS Guarantees," *IEEE Transactions on Wireless Communications*, vol.10, no.7, pp. 2196-2206, 2011. Article (CrossRef Link)

[13] W. Wang, G. Yu and A. Huang, "Cognitive Radio Enhanced Interference Coordination for Femtocell Networks," *IEEE Communications Magazine*, vol.51, no.6, pp. 37-43, 2013. Article (CrossRef Link)

[14] L. G. Yi, Y. M. Lu and T. P. Deng, "Facilitating current terminals accessing to cognitive radio networks," in *Proc. of WiCOM*, pp. 1-4, 2011. Article (CrossRef Link)

[15] T. Weiss, J. Hillenbrand, A. Krohn and F. K. Jondral, "Mutual interference in OFDM-based spectrum pooling systems," in *Proc. of VTC-Spring*, pp. 1873-1877, 2004. Article (CrossRef Link)

[16] G. Bansal, J. Hossain and V. K. Bhargava, "Optimal and suboptimal power allocation

schemes for OFDM-based cognitive radio systems," *IEEE Transactions on Wireless Communications*, vol.7, no.11, pp. 4710-4718, 2008. Article (CrossRef Link)

[17] G. Bansal, O. Duval and F. Gagnon, "Joint overlay and underlay power allocation scheme for OFDM-based cognitive radio systems," in *Proc. of VTC-Spring*, pp. 1-5, 2010. Article (CrossRef Link)

[18] S. P. Boyd and L. Vandenberghe, *Convex Optimization*, Cambridge University Press, 2004. Article (CrossRef Link)

[19] P. T. Boggs and J. W. Tolle, "Sequential quadratic programming," *Acta numerica*, vol.4, no.1, pp. 1-51, 1995. Article (CrossRef Link)

[20] D. W. Sun and B. Y. Zheng, "A Novel Resource Allocation Algorithm in Multi-media Heterogeneous Cognitive OFDM System," *KSII Transactions on Internet and Information Systems*, vol.4, no.5, pp. 691-708, 2010. Article (CrossRef Link)

[21] T. Jiang and Y. Wu, "An overview: Peak-to-Average Power Ratio reduction techniques for OFDM signals," *IEEE Transactions on Broadcasting*, vol.54, no.2, pp. 257-268, 2008. Article (CrossRef Link)

**Leng-Gan Yi** received the M.S. degree from Chongqing University of Posts and Telecommunications, Chongqing, China in communication engineering. He is currently a Ph.D. candidate in the Department of Electronics and Information Engineering, Huazhong University of Science and Technology, Wuhan, China. His research interests include cognitive radio, femtocell networks, radio resource management, game theory, and optimization theory for wireless networks and multimedia communications.

**Yi-Min Lu** is a professor, and Ph.D. supervisor in the Department of Electronics and Information Engineering, Huazhong University of Science and Technology, Wuhan, China. His research interests focus on modern communication technology, multimedia communications, infrared imaging, laser detection and communication.